Phys. Status Solidi C **7**, No. 5, 1301–1304 (2010) / **DOI** 10.1002/pssc.200983123

physica status solidi c
www.pss-c.com
current topics in solid state physics

The microstructure and properties of InN layers

P. Ruterana[1]*, A. L. Syrkin[2], E. Monroy[3], E. Valcheva[4], and K. Kirilov[4]

[1] CIMAP UMR 6176CEA - CNRS-ENSICAEN, 6, Boulevard du Maréchal Juin, 14050 Caen Cedex, France
[2] Technologies and Devices International, Inc., 12214 Plum Orchard Dr, Silver Spring, 20904 MD, USA
[3] CEA/CNRS group ''NanoPhysique et SemiConducteurs'', INAC/SP2M/NPSC, CEA-Grenoble, 17 rue des Martyrs, 38054 Grenoble cedex 9, France
[4] Faculty of Physics, Sofia University, 5 J. Boucher Blvd., 1164 Sofia, Bulgaria

Received 30 September 2009, revised 16 October 2009, accepted 19 October 2009
Published online 11 March 2010

Keywords InN epitaxial growth, TEM characterization, dislocations, optical properties, band gap

* Corresponding author: e-mail pierre.ruterana@ensicaen.fr

A series of InN layers grown by different techniques has been investigated by transmission electron microscopy, photoluminescence and Raman spectroscopy. The polarity is shown to be determined by the underlying GaN template. In these In polar layers, the *c*-screw dislocations density is low and that of *a*-type dislocations is in the high-10^9 cm^{-2} range. The dislocation density tends to decrease towards the surface. Along the first 0.5 µm, and particularly in the samples grown by hydride vapour epitaxy, we observe a large number of stacking faults, which probably contribute to the dislocation density reduction. The optical band gap in MBE and MOVPE samples is between 0.6 and 0.7 eV, but that of the HVPE templates is above 1 eV. Estimations from Raman data show that this behaviour correlates well with the residual carrier concentration.

1 Introduction

InN is still an emerging nitride semiconductor with various interesting properties, such as its high theoretical mobility for electrons (4400 $cm^2V^{-1}s^{-1}$ at 300 K) and its small band gap (~0.7 eV) [1]. In the last few years, it has attracted extensive research interest [1,2] as a promising material for applications like high electron mobility transistors, optical telecommunication devices [3,4] or active media in high-efficiency photovoltaic devices [5,6]. In this sense, an attractive feature of InGaN alloys is their superior resistance against radiation damages in comparison to others solar cells materials (GaAs and InGaP) [5]. InN thin films can also be used for generation of ultrashort THz-radiation pulses with high magnitude compared to other semiconductors [7].

Many of the above-described applications imply band gap engineering from 0.7 eV (InN) to 6.2 eV (AlN) through 3.4 eV(GaN). In this instance, important challenges for the epitaxial growth of highly mismatched materials need to be addressed. Currently, InN thin films of best crystalline quality are obtained by metal organic vapour phase epitaxy (MOVPE) and molecular beam epitaxy (MBE). However, both techniques have low growth rates. An alternate method to synthesize thick template layers is hydride phase epitaxy (HVPE).

On the other hand, the polarity of nitride materials plays a key role in some of their properties like adatom mobility, surface energy, reactivity, or doping/impurity in-diffusion [1]. Hence, its determination is crucial for understanding the material behaviour. Many techniques can be used to determine the polarity of nitride materials. Convergent Beam Electron Diffraction (CBED) is a common method to identify the polarity of crystalline layers. The diameter of the probe can be tuned to a small size (between 1 and 50 nm), which allows accessing areas of the sample with uniform crystalline quality even in highly defective materials. The determination of polarity and thickness using CBED patterns is usually straightforward; it is carried out by comparing the experimental patterns with a series of simulated ones.

However, some limitations of CBED may be relevant for its application to InN layers. First, even with a small probe size, the region of interest must be perfectly defect-free in order to reveal the correct symmetry of the crystal. Therefore, using CBED on materials with a high density of dislocations can be difficult. This is especially

the case in the InN layers under investigation as the dislocation density is in the10^9 cm^{-2} range. In addition, focussing the electron beam is into a very small probe can induce irradiation damage and/or contamination in some materials. In this instance, InN, has been reported to be sensitive to electron beam induced damage [8]. Finally, the effect of temperature on InN CBED patterns has been reported to be strong [9], which could lead to errors in polarity determination. This was investigated using simulations patterns with Debye factors B ranging from 0.0 to 7.0 $Å^2$. It was concluded that the effect of temperature could be less important when the thickness of the specimen is small (~50 nm) [9].

In this paper, we report on the structure and polarity of InN layers grown by various techniques. The CBED results on our samples will be discussed in view of the limitations which have been reported in reference 9. The same samples have been investigated by photoluminescence, absorption and Raman spectroscopy. The results give some insight on the correlation between optical properties and crystallographic defects.

2 Experimental procedure

The investigated samples were grown by HVPE, plasma-assisted MBE and MOVPE on GaN templates (see Table 1). The thickness of the InN layers ranged from 0.15 to 1.2 µm for HVPE samples and from 0.9 to 2 µm for MBE samples, whereas the MOVPE layer was only 150 nm thick. The MBE layers were grown on 4-µm-thick GaN-on-sapphire templates. The InN MOVPE layer was grown in two steps: on top of a thin GaN buffer layer (~50 nm) deposited on sapphire at 550°C and annealed at 1050°C, a nucleation step was carried out at 450°C, and the thick layer growth took place at 520°C. The cross-section transmission electron microscopy (TEM) samples were prepared by mechanical polishing, dimpling and ion-milling using Ar+ ions at 5 kV and a final thinning step at 500 V. During the etching, the sample holder was at the liquid nitrogen temperature. The TEM observations and CBED were performed in a JEOL 2010 microscope

Table 1 The investigated samples, growth methods, and thicknesses of InN and underlying GaN layers

Growth Technique	samples	InN (µm)	GaN (µm)
HVPE	H1	0.5	19
	H2	0.7	7
	H3	1.2	12
MBE	M1	0.9	5
	M2	2	7
MOVPE	O1	0.15	0.05

3 Results

3.1 Microstructure and polarity First, we have performed a microstructural investigation of the InN layers. Figure 1 shows a dark field (DF) micrograph taken with $g=10\bar{1}0$ on the HVPE sample H3. Usually, the dominant defects in nitride layers are threading dislocations (TDs) 10, 11]. However, in this DF image, we observe numerous defects in the basal plane, their density being very high in the first 0.5 µm on top of the GaN interface. Such defects are stacking faults, with a basal component in their displacement vector. The defect density appears to decrease rather drastically towards the layer surface.

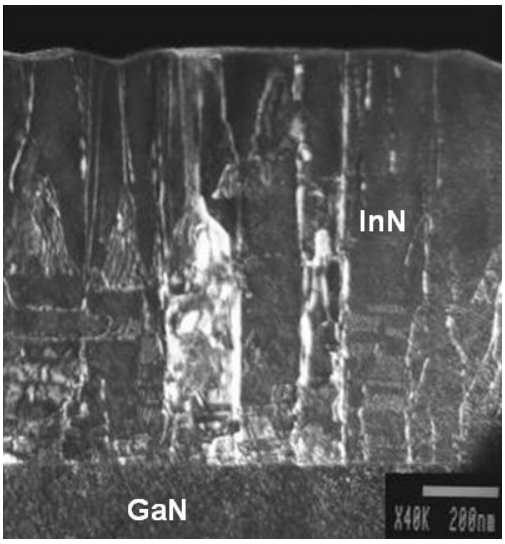

Figure 1 A weak beam micrograph of sample H3, $g=10\bar{1}0$, showing threading dislocations and stacking faults.

As it can be noticed in Fig. 2, the stacking faults exhibited in Fig. 1 are no longer visible when using g=0002 week beam conditions. Therefore, we can conclude that they do not have any component along the **c** axis, and their displacement vector is $1/3 <10\bar{1}0>$, as it corresponds to I2 basal stacking faults [12].

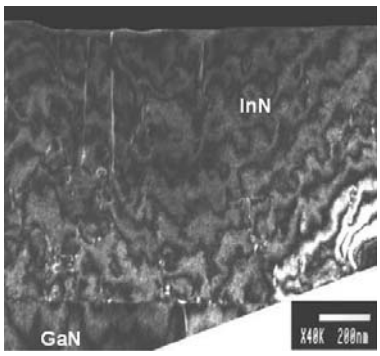

Figure 2 Same area of sample H3, with g=0002, the density of defects with displacement vector along c is significantly smaller.

In the figures above, most of the threading dislocations are visible in the $g=10\bar{1}0$ image (Fig. 1) but not on the g=0002 image (Fig. 2). Hence, they have pure edge character with Burgers vector $\mathbf{b} = \pm 1/3 < 1\bar{1}20 >$. In H3 sample, there is almost one order of magnitude difference in the density of these two types of defects. Table 2 summarizes dislocation density along with residual carriers concentration for the HVPE and MBE samples. The sample exhibits a relatively low density of defects: 5×10^8 cm^{-2}

for pure screw or mixed dislocations, that of the edge dislocations is in the mid 10^9 cm^{-2}. Figure 1 also demonstrates that the interactions between the various defects lead to a reduction of their density towards the surface of the layers.

Table 2 Density of threading dislocations for the HVPE and MBE samples, along with the residual carriers concentration estimated from Raman measurements.

Samples	Type of dislocations (cm^{-2})		Residual carriers concentration (cm^{-3})
	Mixed + screw	edge	
H1	10^9	$2x10^9$ interface 10^9 surface	$4x10^{19}$
H2	10^9	$2x10^9$ interface 10^9 surface	$4x10^{19}$
H3	$5x10^8$	$2x10^9$ interface 10^9 surface	$1.5x10^{19}$
M1	$3x10^8$	$5x10^9$	$1.5x10^{19}$
M2	$3x10^8$	$4x10^9$	-

Inside the MBE layers, due to a smaller density of the basal stacking faults (Fig. 3), there is almost no reduction of the density of the threading dislocations towards the surface of the layers. Such a reduction of the threading dislocation density has been previously reported for MOCVD-grown GaN [11], and more recently in 10 μm thick InN MBE layers [13].

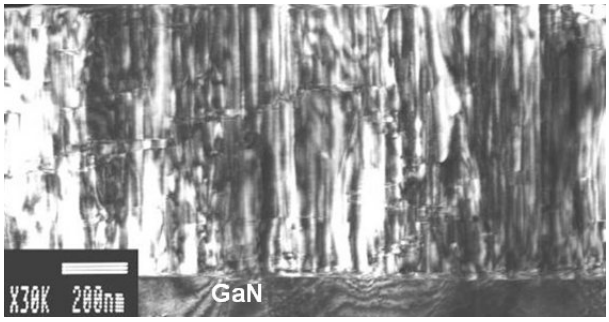

Figure 3 A weak beam micrograph of sample M1, showing edge type threading dislocations, g=10$\bar{1}$0 .

In the MOVPE InN layers under study, the density of c-screw dislocations is rather low, in spite of the small layer thickness (<150 nm), as seen in the weak beam micrograph recorded with g=0002 (Fig. 4).

In all the investigated layers there are neither prismatic stacking faults [14, 15], or inversion domains [16]. This is probably due to the use of low temperature InN buffer layers (MOVPE) or GaN templates with minimum or large surface steps (MBE), respectively [17].

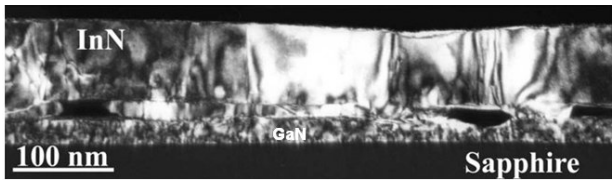

Figure 4 MOVPE InN, on top of sapphire, with a GaN buffer, and a non continuous low-temperature InN layer.

3.2 Layer polarity The substantial reduction of defects within the first 0.5 μm thickness of the HVPE InN layer has proven important for determining the polarity by CBED. Indeed, our various attempts to carry out CBED analysis on thin MOVPE layers (<150 nm) have always been non conclusive. This was more or less in contradiction of the results as reported in reference [9] where it would be much easier and practical to determine the polarity of InN layers with a thickness below or close to 50 nm. We have carried out CBED pattern simulation using the electron microscopy software (EMS) [18], which allows taking into account changes in B factors for the two atoms (In, N) of the wurtzite InN structure. This is equivalent of heating the sample, which may take place during TEM observation. As illustrated in Fig. 5, the variation of the Debye Waller factors modifies the patterns in a highly sensitive way. This means that in InN, any thermal excess will be pointed out easily by CBED patterns. The standard conditions are in column 2 (B:0.5(In), and N(0.2)) as can be obtained from the International Tables of Crystallography.

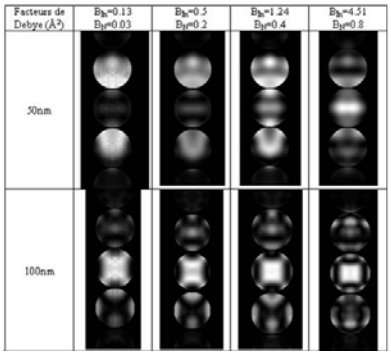

Figure 5 Simulated CBED thickness and B series InN using the EMS system, the deviation from the international tables of crystallography (column 2) changes the patterns.

In HVPE layers, the density of defects showed a substantial decrease with thickness. Therefore, it was possible to record CBED patterns for large thickness spans as can be seen in Fig. 6 (sample H3).

These experimental patterns follow those shown in column 2 of Fig. 5, which means clearly that during observation and TEM sample preparations, the InN layers have not been damaged, and that the thermal heating may not be an issue.

From this thickness series, it is concluded that the absolute polarity of the layers is In, as was driven by the overgrown HVPE GaN templates. In the MBE samples, the obtained results are identical, although the acquisition of thickness series was more limited due to the higher density of defects.

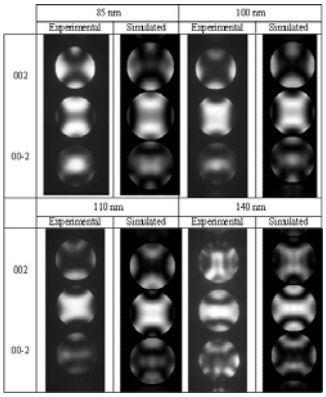

Figure 6 Experimental CBED patterns recorded on sample H3 for various thicknesses, along with simulated ones.

3.3 Optical properties The room temperature photoluminescence (PL) spectra presented in Fig. 7 show higher intensities for the MOVPE (O1) and MBE (M1, M2) layers where the peak maxima are located between 0.6 and 0.7 eV. In the investigated HVPE samples, the PL peaks are beyond 1 eV and the absorption edge onsets can be as far as 1.5 eV(H1, H2). The PL results appear to correlate well with the calculated residual carrier densities estimated from Raman measurements (Table 2).

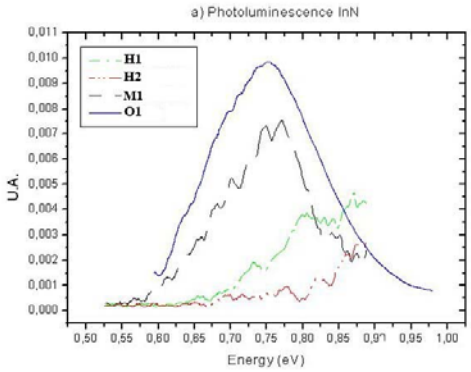

Figure 6 PL emission from 4 representative samples.

4 Discussion and conclusion In the above analysis of InN layers, CBED and conventional TEM show the good crystalline quality of the material, without noticeable foreign phases [19], independently of the growth technique. The layers contain a high density of threading dislocations, which do not seem to play a critical role on their optical properties. As pointed out by other authors, the most important parameter at these still large densities of residual carrier concentration is probably the point defects [20]. This seems to be predominant in HVPE InN layers, where the density of dislocations appears to decrease towards the surface, although the PL emission peak stays always above 1 eV. In fact, on top of these templates which bring about an improved crystalline quality, a regrowth by MBE allows to improve the optical quality [21]. Following the same trend, GaN buffer layers (sample O1) or annealing steps are used in MOVPE [22], which is an indication that the chemical quality, is probably of prime importance, at these still high residual carrier concentrations.

Acknowledgements This work is supported by EU under the project RAINBOW-Grant agreement N°: PITN-GA-2008-213238 and F-1513/05, and the French-Bulgarian bilateral Programme PAI-RILA, project N° DOO2-25/08 and F-1513/05.

References

[1] A.G. Bhuiyan, A. Hashimoto, and A. Yamamoto, J. Appl. Phys. **94**, 2779 (2003).
[2] S.C. Jain, M. Willander, J. Narayan, and R.V. Overstraeten, J. Appl. Phys. **87**, 965 (2000).
[3] J.W. Orton and C.T. Foxon, Rep. Prog. Phys. **61**, 1 (1998).
[4] Hai Lu, W.J. Schaff, and L.F. Eastman, J. Appl. Phys. **96**, 3577 (2004).
[5] J. Wu, W. Walukiewicz, K. M. Yu, W. Shan, J. W. Ager III, E. E. Haller, Hai Lu, William J. Schaff, W.K. Metzger, and S. Kurtz, J. Appl. Phys. **94**, 6477 (2003).
[6] E. Trybus, G. Namkoong, W. Henderson, S. Burnham, W.A. Doolittle, M. Cheung, and A. Cartwright, J. Cryst. Growth **288**, 218 (2006).
[7] R. Ascazubi, I. Wilke, K. Denniston, H. Lu, and W.J. Shaff, Appl. Phys. Lett. **84**, 4810 (2004).
[8] T. M. Smeeton, C. J. Humphreys, J. S. Banard, and M. J. Kappers, J. Mater. Sci. **41**, 2729 (2006).
[9] T. Mitate, S. Mizuno, H. Takahata, R. Kakegawa, T. Matsuoka, and N. Kuwano, Appl. Phys. Lett. **86**, 134103 (2005).
[10] X. H. Wu, L. M. Brown, D. Kapolnek, S. Keller, S. P. Den-Baars, and J. S. Speck, J. Appl. Phys. **80**, 3228 (1996).
[11] V. Potin, P. Ruterana, G. Nouet, R. C. Pond, and H. Morkoc, Phys. Rev. B **61**, 5587 (2000).
[12] V. Potin, P. Ruterana, and G. Nouet: J. Phys.: Condens. Matter **12**, 10301 (2000).
[13] J. Arvanitidis, D. Christofilos, G. A. Kourouklis, A. Delimitis, M. Katsikini, Ph. Komninou, S. Ves, E. Dimakis, and A. Georgakilas, J. Appl. Phys. **100**, 113516 (2006).
[14] P. Vermaut, P. Ruterana, and G. Nouet, Philos. Mag. A **75**, 239 (1997).
[15] J.E. Northrup, Appl. Phys. Lett. **72**, 2316 (1998).
[16] V. Potin, P. Vermaut, P. Ruterana, and G. Nouet, J. Electron. Mater. **27**, 266 (1998).
[17] P. Ruterana, V. Potin, B. Barbaray, and G. Nouet, Philos. Mag. A **80**, 937 (2000).
[18] P. Stadelmann,Ultramicroscopy **21**,131 (1987).
[19] K.M. Yu, Z. Liliental-Weber, W. Walukiewicz, W. Shan, J.W. Ager III, S.X. Li, R.E. Jones, E.E. Haller, H. Lu, and W. J. Schaff, Appl. Phys. Lett. **86**, 071910 (2005).
[20] S.X. Li, K.M. Yu, J. Wu, R.E. Jones, W. Walukiewicz, J.W. AgerIII, W. Shan, E.E. Haller, H. Lu, and W.J. Schaff, Phys. Rev. B **71**,161201R (2005).
[21] A.L. Syrkin, V. Ivantsov, A. Usikov, V.A. Dmitriev, G. Chambard, P. Ruterana A.V. Davydov S.G. Sundaresan, E. Lutsenko, A.V. Mudryi, E.D. Readinger ,G.D. Chern-Met calfe, and M. Wraback, Phys. Status Solidi C 5, 1792 (2008).
[22] P. Ruterana, P. Singh, M. Wojdak, J.L. Doualan, M. Morales, F. Gourbilleau, D. Massimo, W. Richter, and T. Schmidtling, Phys. Status Solidi A **202**(5), 781 (2005).

